TOPICAL REVIEW

Ultrananocrystalline diamond for electronic applications

O A Williams

Institute for Materials Research, Hasselt University, Wetenschapspark 1, B-3590 Diepenbeek, Belgium

E-mail: oliverwilliams@mac.com

Abstract
Ultrananocrystalline diamond is a unique form of carbon with grain sizes in the 3–5 nm region. This nanostructure has profound implications on electronic transport, as ∼10% of carbon is at the grain boundaries. Thus, this material has significant π bonding which governs the majority of the electrical conductivity due to the lower energy gap of π–π^* transitions relative to σ–σ^* transitions. The addition of nitrogen into the gas phase during deposition promotes n-type conductivity, due to the increase in the density of states associated with π bonding. This material is not doped in the conventional sense, and its applications lie in the electrode/metallic conductivity region rather than in the more moderately doped active device regime. This review paper aims to describe the origin and behaviour of the conductivity mechanism, as well as briefly review some applications.

(Some figures in this article are in colour only in the electronic version)

1. Introduction

The discovery of fine grain (3–5 nm) nano-structured carbon films deposited from hydrogen poor plasmas has led to significant research in the properties and applications of this material, named ultrananocrystalline diamond or UNCD [1]. By reducing the relative concentration of atomic hydrogen during the chemical vapour deposition of diamond, it is possible to increase the renucleation rate to the point where all columnar structure is lost. This results in films with grain sizes that are independent of film thicknesses, in stark contrast to conventional diamond deposition. Thus UNCD does not grow in the standard van der Drift regime [2]. The fine grain size of this material results in a very high grain boundary concentration (∼10%), and thus electronic transport phenomena are more complex than those based on classical infinite lattice-based band approximations. Disordered semiconductors also relax the constrictions of the infinite lattice on impurity elements, a particular issue for dense materials such as diamond as it allows impurities of low solubility to be taken up at grain boundaries. The density of UNCD is significantly lower than conventional

diamond due to the high percentage of material at the grain boundaries, and this region may contain many impurities that are highly insoluble in diamond. The enhancement of the grain boundary volume and the simultaneous promotion of n-type conductivity when nitrogen was included in the growth chemistry led to the hypothesis that nitrogen can be incorporated in the grain boundary and produces n-type doping [3]. However, in conventional amorphous and disordered semiconductors, the relaxation of long-range order in fact reduces the possibilities of doping due to impurity atoms being able to take up their preferred chemical bonding. Thus doping is severely constrained in amorphous systems, as donors and acceptors must take substitutional sites for the most efficient doping with the least lattice perturbation.

Substitutional n-type doping of diamond has been problematic principally due to the insolubility of donor atoms into the dense lattice. Phosphorus doping has been the most successful to date, and this dopant has been used to demonstrate diamond p–n junctions [4]. However, the activation energy in diamond is rather high at 0.6 eV [5], leading to low room temperature conductivities. Despite these setbacks, phosphorus remains the n-type dopant of choice

for active electronic devices. Ultrananocrystalline diamond has applications where high conductivities are required at the cost of mobility, due to the disordered nature of the material. These applications include electrochemical electrodes, field emission, heterostructures, etc where the n-type UNCD acts as a source of electrons.

This work details electrical measurements such as the Hall effect over a wide temperature range in an effort to explain the conductivity mechanism in this material. A basic model is proposed using a variant of the established hydrogenated amorphous silicon band structure. Applications for the electronic behaviour of this material are demonstrated and discussed. This review focuses on the electrical transport mechanism of n-type UNCD, and is by no means meant to be exhaustive with regards to applications.

2. Experimental methods

Ultrananocrystalline films were deposited by microwave plasma-enhanced chemical vapour deposition using a hydrogen poor plasma. Prior to deposition, silicon or quartz substrates were ultrasonically seeded in nano-diamond solutions or mechanically dry polished with nano-diamond powders on a polishing cloth. For deposition on single crystal type Ib diamond, no seeding was required. Deposition was monitored by optical emission spectroscopy. Gas-phase chemistry was 1% CH_4 diluted with Ar for intrinsic films. For higher conductivities, nitrogen gas was introduced into the gas phase, the Ar flow rate was reduced to maintain a constant flow and CH_4 concentration. The total percentage of nitrogen in the gas phase is indicated by the sample code, i.e. the 5% N_2 sample was grown with 5% N_2, 94% Ar and 1% CH_4. Thus the nitrogen percentage does not represent a doping concentration or amount of nitrogen in the film. The microwave power was 1400 W and the operating pressure was 150 Torr. All samples were grown at 800 °C as monitored by a thermocouple embedded in the substrate holder.

For electrical measurements, Au contacts were evaporated in the van der Pauw configuration under a base pressure better than 2×10^{-7} mbar. Special care was taken to ensure that there were no conduction paths around the edge or through the substrates leading to erroneous results. Samples were wire bonded in a helium atmosphere-based cryostat and the ohmic nature of the contacts was checked at each temperature point. Hall measurements were performed using a Lakeshore Cryotronics 7504 system, with a magnetic field of 1 T, and Keithley Instrumentation. In order to avoid the convolution of Hall offset voltage and Hall voltage, samples were measured by oscillating the magnetic field between −1 and +1 T with a known period and excitation current. This way, the voltage recorded oscillates with an amplitude twice the Hall voltage. This procedure was applied for several hours at each temperature point from 10 K to 350 K.

Diode heterostructures were fabricated by growing n-type UNCD on single crystal diamond. A highly boron-doped layer was homoepitaxially grown on a commercially available HPHT single crystal diamond. Following this, a thin undoped diamond layer was deposited which had a low concentration of boron due to the background level of the deposition system. On the top of this single crystal sandwich
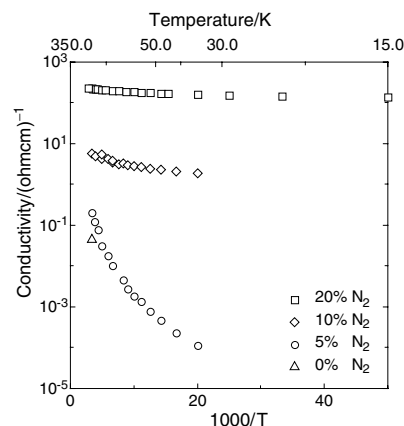

Figure 1. van der Pauw conductivity of UNCD films as a function of reciprocal temperature.

structure, a highly conductive n-type UNCD layer was grown. The mesa structure was fabricated by etching back through the n-type UNCD and lightly p-doped region to the highly boron-doped layer. Thus, an all-carbon rectifier was realized between the highly boron-doped single crystal layer and the n-type UNCD. Measurements were made by spring-loaded point probe contacts direct to the UNCD and highly boron-doped layers in a custom-designed vacuum chamber, with a capability of heating up to 1000 °C.

3. Results

The conductivity of the resulting films as a function of temperature is shown in figure 1 [6]. It can be seen that for all films, the conductivity decreases with decreasing temperature, but with no evidence of a single activation energy of electrical conduction being present. Figure 1 also shows that the conductivity of the films increases with increasing nitrogen in the gas phase. The variation of the conductivity of the films against temperature is far less pronounced for films grown with more nitrogen in the gas phase. For example, the 20% N_2 film conductivity varies less than 25% over the entire temperature range whereas the 5% N_2 film conductivity varies over three orders of magnitude.

Figure 2 shows the Hall voltage oscillations resulting from the oscillation of the magnetic field. Figure 2(a) shows the p-type diamond (control) case, where the Hall signal is 180° out of phase with the magnetic field. It can be seen that in figure 2(b), the Hall signal is in phase with the magnetic field, hence 180° out of phase with the p-type diamond, i.e. opposite polarity and n-type. Both figures 2(a) and (b) show a drift in the Hall signal due to temperature variations, contact drift and atmospheric effects, as previously reported [7]. The Hall signal in these films shows clear n-type behaviour deconvoluted from the Hall offset voltage. The n-type nature of all films was confirmed by the positive electromotive force at the hot probe with respect to the cold probe during Seebeck/thermopower measurements.

The sheet carrier concentrations of the UNCD films as determined from the aforementioned Hall procedure are plotted as a function of temperature in figure 3. It was only possible to measure carrier concentrations in films grown with
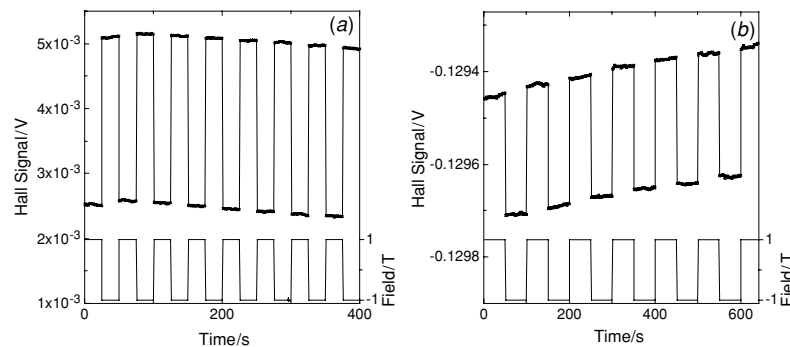
Figure 2. Hall sweeps of (*a*) high mobility p-type diamond and (*b*) n-type UNCD [36].
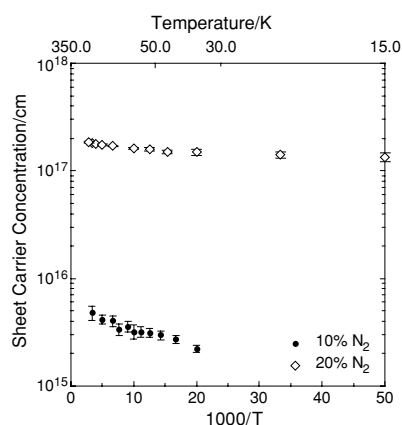

Figure 3. Sheet carrier concentrations of UNCD films as a function of temperature [36].
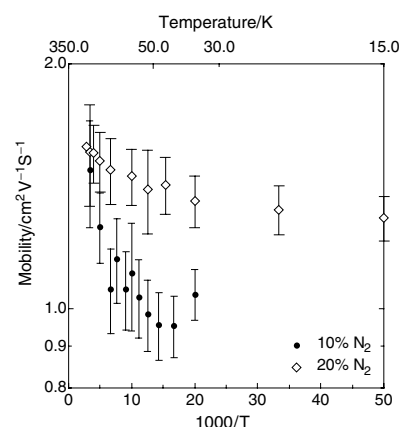

Figure 4. Hall mobilities of UNCD films as a function of reciprocal temperature [36].

Figure 5. van der Pauw conductivity of UNCD films as a function of $T^{-1/4}$.

10% N_2 and above in the gas phase. It can be seen from this figure that sheet carrier concentrations of both the 10% and 20% N_2 films reduce with reducing temperature, but are largely temperature insensitive. At room temperature the 20% N_2 sample has a sheet carrier concentration of $\sim 2 \times 10^{17}$ cm^{-2} and the 10% sample 5×10^{15} cm^{-2}. These films are around 2–3 μm thick, yielding bulk carrier densities in the 10^{19}–10^{21} cm^{-3} region, which is an extremely high free-electron concentration for diamond at room temperature. As with the conductivity of these films, the sheet carrier concentration is more variable against temperature for films grown with less nitrogen in the gas phase. Figure 4 displays the carrier mobility values of these films as a function of reciprocal temperature. The room temperature values of UNCD mobilities are around 1–2 cm^2 V^{-1} s^{-1} and decrease with decreasing temperature. The reduction in mobility with reducing temperature is more pronounced in the 10% N_2 sample than the 20% sample, but neither sample varies more than 50% over the entire temperature range.

Figure 5 shows the van der Pauw conductivity values of figure 1 replotted against $T^{-1/4}$ to investigate the possibility of variable range hopping in three dimensions. It can be seen that in this figure, the data of all samples seem to correlate very well especially at lower temperatures, resulting in a straight line for all films with reducing gradient as the nitrogen content is increased. The 10% and 20% N_2 films show very shallow gradients against $T^{-1/4}$. Secondary ion mass spectroscopy (SIMS) data for films grown with nitrogen are shown in
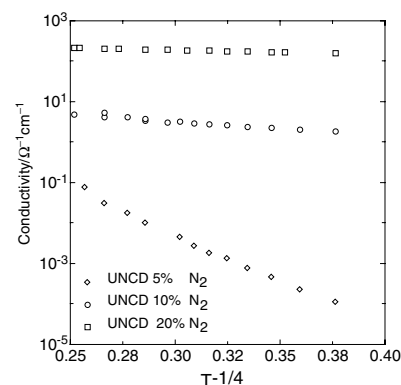
figure 6, the data taken from Bhattacharyya *et al* [3]. It can be clearly seen from this figure that the nitrogen content in the UNCD films increases with increasing nitrogen in the gas phase. However, it is also visible from this figure that the total nitrogen concentration in the films is below the free-carrier concentration of these films. It is also clear that the total nitrogen concentration in these films only varies by a factor of 4 between all of the films whereas the conductivity varies over four orders of magnitude in these same films.

In figure 7, TEM images of films grown with 1% N_2 and 20% N_2 are shown, the figure again reprinted from
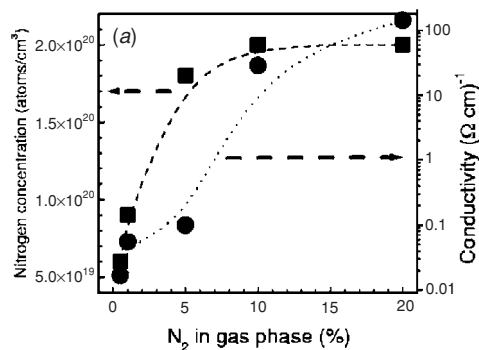
Figure 6. Secondary ion mass spectroscopy of UNCD films as a function of nitrogen concentration within the gas phase [3], reprinted with permission from AIP.
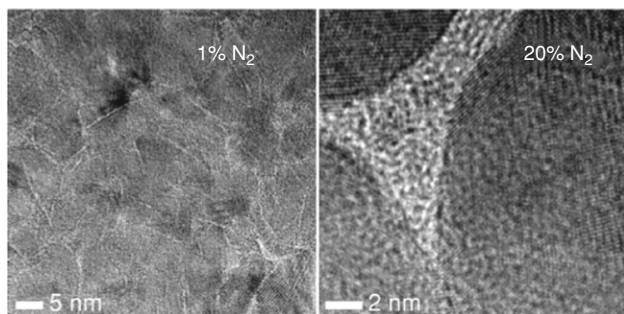

Figure 7. Transmission electron micrograph images of UNCD films [3], reprinted with permission from AIP.

Bhattacharyya *et al* [3]. This figure shows that for 1% N_2 films, the structure is fundamentally crystalline with grain size within the 3–5 nm regime, as previously reported for UNCD films [1]. With the addition of high quantities of nitrogen into the gas phase however, the grain boundary regions between grains significantly broaden. These regions are significantly brighter in the TEM image due to their enhanced conductivity, and are fundamentally not crystalline.

In figure 8 a schematic of a diamond/UNCD heterostructure is shown. This meta-structure comprises a highly doped (p+) boron layer grown homoepitaxially on a type Ib single crystal diamond. On the top of this layer, a thin lightly doped (p−) boron layer is grown followed by n+ UNCD. A mesa structure is defined by etching through the UNCD and lightly doped boron layer to reach the p+ layer. The device is measured between this p+ layer and the n+ UNCD layer. The *I/V* characteristics of this heterostructure are shown in figure 9. This heterostructure shows very high rectification ratios at room temperature. At elevated temperatures the forward bias current increases and the reverse bias current remains constant; hence the rectification rises with increasing temperature up to 300 °C. At higher temperatures the rectification ratio decreases due to reverse bias leakage. This heterostructure operates at temperatures over 900 °C and can be repeatedly temperature cycled between room temperature and 1000 °C with no degradation in performance. Figure 10 shows the forward bias region of this rectifier as a function of temperature. Figure 10(*a*) shows that this diode has a high ideality factor $n = 3.0$, but it is still possible to
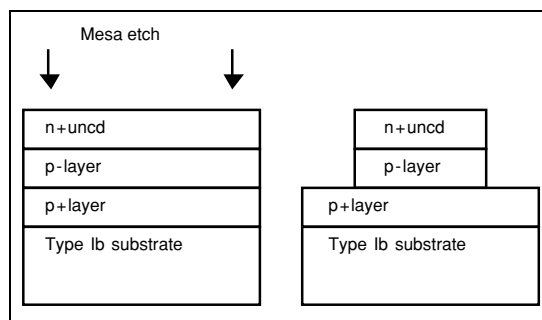
Figure 8. Schematic of an UNCD/single crystal diamond heterostructure.
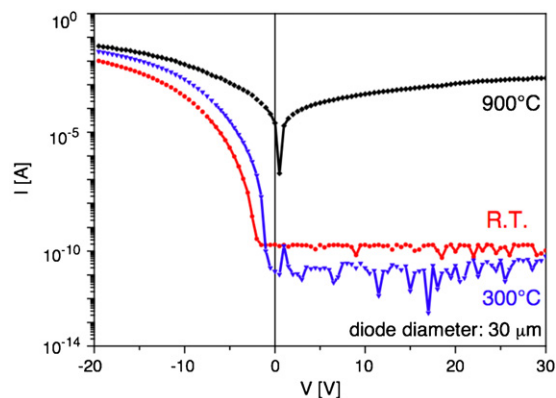

Figure 9. Current/voltage plot of the UNCD/single crystal diamond heterostructure [37], reprinted with permission from Elsevier.

obtain an extrapolated intercept to determine the interfacial barrier potential of 0.72 eV as shown in figure 10(*b*).

4. Discussion

Gas phases with higher nitrogen levels result in films with higher conductivities, as shown in figure 1. This figure shows no evidence of a single activation energy of electrical conduction for any of the films, and thus the conductivity behaviour as a function of temperature is not reminiscent of conventional doping, i.e. a distinct energy level below the conduction band minimum. The increase in conductivity with increased nitrogen concentration in the gas phase is as might be expected for a conventional dopant, but the levels of nitrogen here are far too high for conventional doping. The films with increased conductivity also show less sensitivity to temperature which is consistent with high doping levels or a high density of states associated with defects.

Figures 2(*a*) and (*b*), combined with thermopower/Seebeck measurements, show that this material is unequivocally n-type. The high carrier concentrations make the magnitude of the Hall voltage rather small relative to the offset voltage, but a clear signal is visible with a slight background drift due to temperature and contact drift. Amorphous and disordered materials have been known on occasion to yield the opposite polarity of the Hall voltage to the free-carrier type by Hall effect, a phenomenon termed the 'sign anomaly' [8]. However, this effect is more often
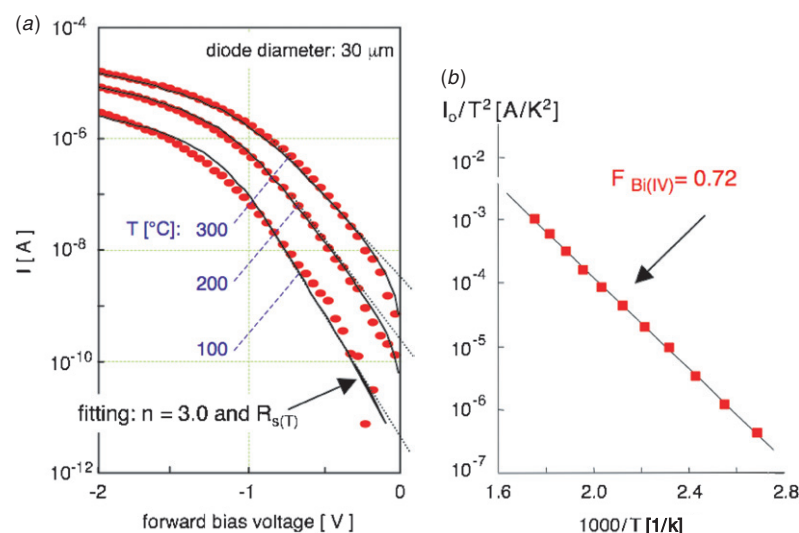
Figure 10. Forward bias current/voltage characteristics as a function of temperature [37], reprinted with permission from Elsevier.

found in amorphous materials, and when the grain size is <3 nm and carrier mobilities are $<10^{-1}$ V^{-1} s^{-1} [9], i.e. an order of magnitude lower than those shown here. The carrier densities observed in these films are very high. Assuming a thickness of around 2 μm, the 20% N$_2$ sample has a carrier concentration of 10^{21} cm^{-3}. This is extremely high for diamond, and never before observed at room temperature for n-type diamond. More common values for phosphorus-doped diamond at room temperature are around 10^{12} cm^{-3} [10] due to the high activation energy of 0.6 eV. The variation of carrier concentration against temperature is semi-metallic for both the 10% and 20% N$_2$ samples, the greater variation for the film with lower carrier concentration as expected. The low mobility values in figure 4 are low due to the nanoscale grain sizes and the high carrier concentrations exhibited in these films.

As the conductivity behaviour of these films does not follow Arrhenius-type behaviour as shown in figure 1, the conductivity is replotted in figure 5 to the standard Mott–Davies hopping in three dimensions, that is to T$^{-1/4}$. It can be seen from this plot that the correlation is rather good, especially for samples grown with lower nitrogen concentrations and in the lower temperature regime. Thus, it is very probable that the conductivity mechanism is some kind of hopping at these lower concentrations. This result also explains the lack of a strong Hall signal in films grown with low nitrogen contents, as hopping is a low mobility process.

Figure 6 shows that the nitrogen concentration within the UNCD films as measured by SIMS does not correlate with the free-electron concentration. When compared with figure 3, it can be seen that for a 20% N$_2$ film, the carrier concentration is an order of magnitude higher than the nitrogen concentration. This point is crucial, as it means that nitrogen within UNCD films cannot act as a substitutional dopant with low activation energy. With substitutional doping the free-carrier concentration can be lower than the doping concentration but not higher as in this case. Nitrogen forms a very deep donor in single crystal diamond [11] and is more appropriately viewed as a trap or defect than a dopant.

Nitrogen also forms complexes with vacancies [12], but none of these defects in conventional diamond result in shallow donor levels and nitrogen is generally considered detrimental to electronic-grade diamond growth. For example, the state of the art in single crystal diamond growth has nitrogen levels $<1 \times 10^{15}$ cm^{-3} [13].

It has been suggested that it may be easier to dope nanocrystalline diamond due to its lower density and the relaxation of long-range order, but it should be pointed out that this in fact makes doping more difficult. Substitutional doping is the replacement of lattice atoms with atoms from a neighbouring group which when ionized generate a free electron or hole. This relies on the long-range order of the lattice to force the alien atom into the lattice configuration and generate the free carrier. In amorphous and highly disordered semiconductors this long-range order is absent, and this allows impurity atoms to take up their own desired chemical bonding. Thus, impurity atoms do not necessarily contribute to conductivity. This phenomenon led to a prediction of the atom coordination by Mott, which is known as the $8 - N$ rule [14, 15]. This rule states that the optimum number of covalent bonds Z for elements is $8 - N$ for $N \geqslant 4$ and $Z = N$ for $N < 4$, where N is the number of valence electrons. Thus for the case of nitrogen in diamond, for the crystalline lattice-constrained case the atom becomes four-fold coordinated and releases an electron into the conduction band as it is not involved in bonding, albeit with a high activation energy. However, the $8 - N$ rule predicts that nitrogen will be three-fold coordinated in amorphous/disordered regions with the remaining electrons in a lone pair configuration and inactive as an electronic dopant. Theoretical studies have shown that this is exactly what happens in UNCD, with nitrogen relaxed to three-fold or two-fold coordinated sites in the grain boundary [16]. The remaining lone pair is predicted to generate energy level near the valance band maximum rather than near the conduction band minimum [16].

It has been shown that nitrogen does not reside within the core of nano-diamond particles in four-fold configuration; thus it is unlikely to act as a donor in UNCD films with similar

grain sizes [17]. In fact it has been shown theoretically that all grain boundary sites are preferred over the diamond bulk for nitrogen substitution [16]. Therefore, it is unlikely that nitrogen produces conductivity in UNCD films by conventional doping mechanisms. It must then be considered how the addition of nitrogen into the gas phase generates conductivity. The increase in the conductivity of UNCD films with added nitrogen is reminiscent of nitrogenated ta-C and other DLCs [18]. These materials are fundamentally disordered or in fact in this particular reference amorphous, and the effect of nitrogen on conductivity is more related to structure than to doping. The grain boundaries of UNCD are also heavily disordered and look amorphous in figure 7. It is also clear from the contrast of figure 7 that the grain boundaries are more conductive than the grain interiors, and thus when considering electronic transport in UNCD one is primarily interested in the grain boundary regions.

The main difference in the electronic structure of disordered materials in comparison with their single crystal counterparts is due to their lack of long-range order. This lack of long-range order results in band tailing, i.e. the broadening of the conduction and valence bands into the forbidden gap. However, the gap between these bands is still large and not the origin of the conductivity is reported here. In disordered carbon systems, the electrical properties are dominated by π bonding as the energy spacing of $\pi-\pi^*$ transitions is much lower than the $\sigma-\sigma^*$ transitions more associated with the conventional diamond bandgap [19]. The grain boundary content of UNCD films grown without nitrogen is around 10% and increases with the addition of nitrogen in the gas phase. UNCD films grown without nitrogen have an sp^2 content of around 5% and higher sp^2 levels have also been observed in films grown with nitrogen in the gas phase by NEXAFS [20]. Therefore it is reasonable to infer that the increased conductivity is due to the increase in sp^2 bonding and that this is situated at the grain boundary as figure 7 suggests. Thus, the effect of the addition of nitrogen into the gas phase is to broaden the π and π^* bands, reducing the forbidden energy gap and transparency of the UNCD film [21, 22].

The predominant conductivity mechanism is therefore probably hopping at low temperatures as suggested in figure 5 and thermally activated transport in an impurity/defect band at higher temperatures. The effect of the nitrogen addition should be viewed as more indirect than doping, that is, nitrogen forces structural changes during the deposition of UNCD, and these lead to enhanced sp^2 bonding which ultimately determines the conductivity of the resulting film. These effects are not new in the field of carbon. Both ta-C and DLC exhibit enhanced conductivity when deposited with nitrogen in the gas phase [18]. In ta-C, the addition of nitrogen leads to a shift in the Fermi level towards the conduction band, but as mentioned above, the predominant reason for the increase in conductivity is the high density of states in the bandgap. One can explain the conductivity behaviour at low nitrogen levels as a hopping transport mechanism similar to that seen in figure 5. However, at higher nitrogen levels a CN alloy forms in ta-C and the optical gap drops considerably. This effect of the increase in optical absorption with increasing nitrogen is also seen in UNCD [22]. This is again due to states within the bandgap, and these are mainly due to sp^2 bonding. Thus, as in ta-C, there is an inverse correlation between conductivity and

transparency with UNCD, with conductivity also proportional to sp^2 content. It should be noted that the addition of small quantities of hydrogen to the gas phase significantly increases transparency and reduces conductivity. This can be seen as the reduction of dangling bond states within the bandgap as in the case of hydrogenated amorphous silicon. There is also an enhanced etching of amorphous carbon due to increased atomic hydrogen in the plasma, resulting in a reduction in sp^2 states within the bandgap. Higher nitrogen levels in ta-C result in the formation of a CN alloy, and it is reasonable to speculate that the grain boundary regions in UNCD grown with high nitrogen content in the gas phase may be some kind of amorphous CN or nitrogenated ta-C material.

The problem with this hypothesis is the relatively high mobility recorded, but it should be noted that Hall effect measurements are difficult to interpret in two-phase systems like here, with the conductivity in the grain boundaries [23]. It is more appropriate to view the conductivity mechanism at high nitrogen contents in view of percolation theory, but the data here are inadequate for a rigorous treatment. Thus the conductivity of the UNCD film is determined by sp^2 states within the bandgap originating at the grain boundary regions, and their enhancement with nitrogen addition in the gas phase.

This conductivity mechanism is of limited use for active electronic devices as it results in high carrier concentrations with low mobilities, leaving it difficult to form depletion regions, etc required for rectification and modulation. This means that all metal UNCD contacts will be ohmic regardless of the metals' work function, as any Schottky barrier will be tunnelled through easily due to the high doping level. This has been confirmed experimentally [24], and thus UNCD is limited to devices that operate in the near-metallic regime.

One such area where UNCD is of use is as an electrochemical electrode. Electrochemistry is a strong application of diamond especially in water purification [25], due to the wide electrochemical window, high signal-to-noise ratios and long-term stability. UNCD is a very effective electrochemical electrode due to the aforementioned high carrier concentrations, high conductivities and the chemical resilience of diamond [26]. Generally, boron-doped diamond is used in these applications [27], but UNCD is a possible alternative for some applications. The electrochemical window of UNCD is slightly smaller than boron-doped diamond due to its higher sp^2 content, and the background current is also slightly higher [26]. This grain boundary carbon is also redox active [26], and growth of diamond or UNCD with nitrogen increases these sites which reduce the electrochemical window [28]. Despite these limitations UNCD can be used as an effective electrochemical electrode, and may have some advantages for particular applications [29].

Another area where highly conductive UNCD is of use is in field emission, where smooth conformal coatings of UNCD on silicon substrates have exhibited emission thresholds as low as 2 V μm^{-1} [30, 31]. This value rivals carbon nanotubes and is due to the grain boundary conduction mechanism mentioned above. The high density of states within the bandgap significantly reduces the potential barrier for field-emitted electrons. These grain boundary regions also provide a conductive path to the UNCD/vacuum interface, which is surrounded by non-conductive sp^3 regions. As these

grain boundaries are rather narrow, they provide strong field enhancement in the local electric field at the interface. This behaviour is similar to that reported in amorphous carbon films, where it was found that the electron field emission originated from small sp^2 regions in an sp^3 matrix [32]. The optimum size of sp^2 regions has been shown to be $\leqslant 1$nm, which is comparable with the grain boundaries of UNCD shown in figure 7. This is a significant advantage of UNCD as the field enhancement factor can be very high without manipulation of the topography. This particular intrinsic property of UNCD could prove instrumental in the enhancement of lateral field emission devices [33, 34]. It seems, then, that the inhomogeneous nature of UNCD conductivity is not a problem for all applications.

The heterostructure diode shown in figures 9 and 10 makes use of the electrode properties of UNCD. Basically, this device is an all-carbon rectifier, with UNCD acting as a metal-like electrode. At first look, it is tempting to view this device as a p–n junction, but for the aforementioned points on the UNCD conductivity mechanism, i.e. the reduced bandgap, midband states, etc, it is more appropriate to view this device as a Schottky diode. This is also evident in the low Schottky barrier height recorded, i.e. it is much lower than that of a single crystal diamond p–n junction with a nitrogen doped n-type region [35]. The interface and thus the barrier height are dominated by the single crystal diamond/UNCD grain boundary interface, the grains of the UNCD having a much lesser effect on the Schottky barrier height. As the interface is all carbon, the device has extreme temperature stability and can be operated under temperature regimes where a metal electrode would fail due to lattice mismatch and differences in thermal expansion coefficient. This device structure and those based on the same principles of an all-carbon active device region could have applications in very high-temperature regimes and harsh environments where other materials simply cannot operate.

5. Conclusions

Ultrananocrystalline diamond can be made highly conductive by the addition of nitrogen into the gas phase during deposition and this conductivity is n-type. However, this conductivity is not due to doping, but due to the manipulation of the nanostructure of the material, leading to enhanced sp^2 regions and midgap states. This leads to low mobility hopping-type conduction processes and impurity band conduction, with very high carrier concentrations and low mobilities. Thus, this conductivity mechanism is of little use in active electronics, where the formation of depletion regions is crucial to device modulation and rectification. However, UNCD can be highly useful where high carrier concentrations are required, such as in electrochemical electrodes, field emission, heterostructures, high-temperature stable ohmic contacts, etc.

References

[1] Gruen D M 1999 Nanocrystalline diamond films *Ann. Rev. Mater. Sci.* **29** 211–59
[2] van der Drift A 1967 *Philips Res. Rep.* **22** 267
[3] Bhattacharyya S *et al* 2001 Synthesis and characterization of highly-conducting nitrogen- doped ultrananocrystalline diamond films *Appl. Phys. Lett.* **79** 1441–3
[4] Koizumi S, Watanabe K, Hasegawa F and Kanda H 2001 Ultraviolet emission from a diamond pn junction *Science* **292** 1899–901
[5] Nesladek M 2005 Conventional n-type doping in diamond: state of the art and recent progress *Semicond. Sci. Technol.* **20** R19–27
[6] Williams O A, Zimmermann T, Kubovic M, Denisenko A, Kohn E, Jackman R B and Gruen D M 2005 Electronic properties and applications of ultrananocrystalline diamond *Synthesis, Properties and Applications of Ultrananocrystalline Diamond* ed D M Gruen, O A Shenderova and A Y Vul (Berlin: Springer) pp 373–82
[7] Williams O A and Jackman R B 2003 Surface conductivity on hydrogen terminated diamond *Semicond. Sci. Technol.* **18** S34–40
[8] Nebel C E and Street R A 1993 Hall experiments and interpretation in a-Si-H and a-Sic-H *J. Non-Cryst. Solids* **166** 449–52
[9] Nebel C E, Rother M, Stutzmann M, Summonte C and Heintze M 1996 The sign of the Hall effect in hydrogenated amorphous and disordered crystalline silicon *Phil. Mag. Lett.* **74** 455–63
[10] Koizumi S, Teraji T and Kanda H 2000 Phosphorus-doped chemical vapor deposition of diamond *Diam. Relat. Mater.* **9** 935–40
[11] Davies G 1977 *The Optical Properties of Diamond* (New York, USA: Dekker)
[12] Davies G, Lawson S C, Collins A T, Mainwood A and Sharp S J 1992 Vacancy-related centers in diamond *Phys. Rev. B* **46** 13157–70
[13] Isberg J, Hammersberg J, Johansson E, Wikstrom T, Twitchen D J, Whitehead A J, Coe S E and Scarsbrook G A 2002 High carrier mobility in single-crystal plasma-deposited diamond *Science* **297** 1670–2
[14] Mott N and Davies E 1979 *Electronic Processes in Non-Crystalline Materials* (Oxford: Oxford University Press)
[15] Street R A 1991 *Hydrogenated Amorphous Silicon* (Cambridge: Cambridge University Press)
[16] Zapol P, Sternberg M, Curtiss L A, Frauenheim T and Gruen D M 2002 Tight-binding molecular-dynamics simulation of impurities in ultrananocrystalline diamond grain boundaries *Phys. Rev. B* **65** 045403
[17] Barnard A S and Sternberg M 2005 Substitutional nitrogen in nanodiamond and bucky-diamond particles *J. Phys. Chem. B* **109** 17107–12
[18] Kleinsorge B, Ferrari A C, Robertson J and Milne W I 2000 Influence of nitrogen and temperature on the deposition of tetrahedrally bonded amorphous carbon *J. Appl. Phys.* **88** 1149–57
[19] Robertson J 2003 Electronic and atomic structure of diamond-like carbon *Semicond. Sci. Technol.* **18** S12–9
[20] Birrell J, Gerbi J E, Auciello O, Gibson J M, Gruen D M and Carlisle J A 2003 Bonding structure in nitrogen doped ultrananocrystalline diamond *J. Appl. Phys.* **93** 5606–12
[21] Nesladek M, Meykens K, Stals L M, Vanecek M and Rosa J 1996 Origin of characteristic subgap optical absorption in CVD diamond films *Phys. Rev. B* **54** 5552–61
[22] Achatz P, Garrido J A, Stutzmann M, Williams O A, Gruen D M, Kromka A and Steinmuller D 2006 Optical properties of nanocrystalline diamond thin films *Appl. Phys. Lett.* **88** 101908
[23] Mares J J, Hubik P, Kristofik J, Kindl D, Fanta M, Nesladek M, Williams O and Gruen D M 2006 Weak localization in ultrananocrystalline diamond *Appl. Phys. Lett.* **88** 92107
[24] Gerbi J E, Auciello O, Birrell J, Gruen D M, Alphenaar B W and Carlisle J A 2003 Electrical contacts to

ultrananocrystalline diamond *Appl. Phys. Lett.* **83** 2001–3

[25] Furuta T, Tanaka H, Nishiki Y, Pupunat L, Haenni W and Rychen P 2004 Legionella inactivation with diamond electrodes *Diam. Relat. Mater.* **13** 2016–9

[26] Fausett B, Granger M C, Hupert M L, Wang J, Swain G M and Gruen D M 2000 The electrochemical properties of nanocrystalline diamond thin-films deposited from C-60/argon and methane/nitrogen gas mixtures *Electroanalysis* **12** 7–15

[27] Hupert M, Muck A, Wang R, Stotter J, Cvackova Z, Haymond S, Show Y and Swain G M 2003 Conductive diamond thin-films in electrochemistry *Diam. Relat. Mater.* **12** 1940–9

[28] Gerger I and Haubner R 2005 Cyclic voltammetry measurements on boron- and nitrogen-doped diamond layers *Diam. Relat. Mater.* **14** 369–74

[29] Hian L C, Grehan K J, Compton R G, Foord J S and Marken F 2003 Influence of thin film properties on the electrochemical performance of diamond electrodes *Diam. Relat. Mater.* **12** 590–5

[30] Krauss A R *et al* 2001 Electron field emission for ultrananocrystalline diamond films *J. Appl. Phys.* **89** 2958–67

[31] Corrigan T D, Gruen D M, Krauss A R, Zapol P and Chang R P H 2002 The effect of nitrogen addition to Ar/CH$_4$ plasmas on the growth, morphology and field emission of ultrananocrystalline diamond *Diam. Relat. Mater.* **11** 43–8

[32] Ilie A, Ferrari A C, Yagi T, Rodil S E, Robertson J, Barborini E and Milani P 2001 Role of sp(2) phase in field emission from nanostructured carbons *J. Appl. Phys.* **90** 2024–32

[33] Subramanian K, Kang W P, Davidson J L, Jarvis J D, Hofmeister W H, Choi B K and Howell M 2006 Geometrical field enhancement on micropatterned nanodiamond film for electron emissions *Diam. Relat. Mater.* **15** 417–25

[34] Subramanian K, Kang W P, Davidson J L, Hofmeister W H, Choi B K and Howell M 2005 Nanodiamond planar lateral field emission diode *Diam. Relat. Mater.* **14** 2099–104

[35] Aleksov A, Denisenko A and Kohn E 2000 Prospects of bipolar diamond devices *Solid-State Electron.* **44** 369–75

[36] Williams O A, Curat S, Gerbi J E, Gruen D M and Jackman R B 2004 n-type conductivity in ultrananocrystalline diamond films *Appl. Phys. Lett.* **85** 1680–2

[37] Zimmermann T, Kubovic M, Denisenko A, Janischowsky K, Williams O A, Gruen D M and Kohn E 2005 Ultra-nano-crystalline/single crystal diamond heterostructure diode *Diam. Relat. Mater.* **14** 416–20